

Simulation of flash flood peaks in a small and steep catchment using rain-on-grid technique

Nitesh Godara  | Oddbjørn Bruland | Knut Alfredsen

Department of Civil and Environmental Engineering, Norwegian University of Science and Technology, 7491 Trondheim, Norway

Correspondence

Nitesh Godara, Department of Civil and Environmental Engineering, Norwegian University of Science and Technology, 7491 Trondheim, Norway.
Email: nitesh.godara@ntnu.no

Abstract

The frequency of extreme events is increasing as the consequences of climate change. In steep terrains, flash floods with high-flow velocities induce erosion and sedimentation with potentially disastrous changes of flood path. Hence, the analysis of flash floods in steep terrains in terms of inundation area and flow-velocity to identify critical points becomes more important. The output of a flood simulation with a traditional hydrologic model provides the flood hydrograph which must be combined with a hydraulic model for downstream consequences. In small and steep catchments, the inflow contribution from every section of the water course can be important to determine where critical conditions may arise. In this study, rain-on-grid technique in the hydraulic model Telemac-2D is used to simulate flash-flood peaks with spatially distributed precipitation as input in a small and steep catchment in western Norway. Seven events were simulated and sensitivity tests on parameters were conducted. A 200-year design flood was simulated to show the potential consequences in the catchment. The results show that calibrated models can satisfactorily reproduce peak flows and produce relevant information about water velocities and inundation which decision makers can use for mitigation measures. The paper explores the benefits and limitations through a description of model construction, calibration, and test of sensitivities.

KEYWORDS

hydrological modelling, rainfall-runoff modeling, TELEMAC-2D, hydraulic modelling, climate change adaption

1 | INTRODUCTION

The frequency and severity of extreme events are increasing as the consequences of climate change (Costache et al., 2022; Seneviratne et al., 2021). According to the World Meteorological Organization (WMO, 2021), floods are the third largest hazard in terms of human losses (58,700 deaths) and second largest in terms of economic

losses (US\$115 billion). Among all the flooding types, flash floods are one of the most disastrous natural hazards causing significant loss of life and economy throughout the world and Europe (Adnan et al., 2019; Gaume et al., 2009; Hu et al., 2018; Merz et al., 2021; Saharia et al., 2017; Trigo et al., 2016; Zhai et al., 2021). Hence, the analysis of flash floods is crucial to predict and prevent their consequences. Such studies are also necessary

This is an open access article under the terms of the [Creative Commons Attribution-NonCommercial License](https://creativecommons.org/licenses/by-nc/4.0/), which permits use, distribution and reproduction in any medium, provided the original work is properly cited and is not used for commercial purposes.

© 2023 The Authors. *Journal of Flood Risk Management* published by Chartered Institution of Water and Environmental Management and John Wiley & Sons Ltd.

for the development of decision support tools for efficient flood mitigation works and for planning infrastructure against flash flood damages, the design of hydraulic structures (Kayan et al., 2021) and watershed management. Flash floods are usually triggered by heavy rainfall events in a short period or/and contribution from sudden snow melt because of high temperature or/and rainfall on the snow (Zhai et al., 2021). The catchment response time is even shorter in small and steep mountainous catchments (Bruland, 2020) as compared to the larger and flatter catchments. Small catchments are frequently affected by flash floods (Bryndal et al., 2017) specially when the slope is also high (Costache et al., 2021). The high precipitation intensity in such catchments leads to extreme peak flows and high flow velocities (Jia et al., 2018) sometimes causing landslides due to high shear stresses (Moraru et al., 2021). Flash floods can lead to erosion and sedimentation which can cause the river channels to change its path (Roald, 2019). Hence, the current study focuses on the flash flood analysis in small and steep catchments.

The impact is enhanced by human activities such as concretizing of the natural soil decreasing its water retention capacity, settlement in flood plains changing land cover and land use (Boithias et al., 2017). Damages due to flash floods are not only dependent on the rainfall intensity and duration, catchment and water course properties also play a significant role (Merz et al., 2010). Water velocities, erosion, and sedimentation can cause severe problems which need to be addressed in areal and infrastructure planning (Kreibich et al., 2009). Shand et al. (2011) focuses on the safety of people and vehicles in a floodplain. Their study shows that the product of water velocities and water depth should be between 0.4 and 0.7 m²/s to keep pedestrians and vehicles safe, respectively. Smith (1994) presents a relation between critical velocity and depth for building failure. The Norwegian Building Acts and Regulations (DiBK, 2017) includes a paragraph saying that if the product of water velocities and water depth exceeds 2 m²/s, the risk level is higher compared to other areas. Hence, it is important to analyze both the response of the catchment and the river to understand floods and their consequences and how to implement this in societal planning.

Most of the hydraulic models need to have a hydrograph from a hydrologic model as a boundary condition to assess flood damages. Whereas most of the traditional hydrologic models only give the hydrographs as an output commonly at the outlet of the catchment, but do not present the consequences of those peaks such as the velocity, water depths, and shear stresses along the water course. If hydrologic and hydraulic models can be integrated in an efficient way, it can be the solution to assess

catchment response and hydraulic impacts and thereby the consequences of floods. Many studies have loosely coupled the models, also called the offline coupling (Felder et al., 2017; Nguyen et al., 2016), in which the output from the hydrologic model is used as the input to the hydrodynamic model and set as a boundary condition before the hydrodynamic model runs. Therefore, the timely delivery of output from the hydrological model is required to get the hydraulic models running and getting the results in time. Moreover, the offline coupling requires the separate calibration of two models which makes it even more time-consuming (Li et al., 2021). Also, there is the issue of where in the catchment this input boundary condition should be set in the hydraulic model. Sometimes due to many tributaries, more than one boundary condition is required. In addition to this, there is always some residual flow along the river from the catchment or the water from small tributaries which is difficult to estimate and add in the hydraulic model calculations.

To overcome these challenges and to remove the hassle of offline-coupling of the two kinds of model, the direct rainfall method (DRM), also referred as the rain-on-grid (RoG) technique, is used. This technique allows the user to apply the input rainfall directly on the grid cells of a 2D hydraulic model (David & Schmalz, 2020; Hall, 2015). Hall (2015) used RoG on a portion of a 185 km² big flat catchment with a grid size of 20 m, and for the rest of the catchment, a traditional hydrological model was used to reduce the total computational time. The study mentions some limitations of using the RoG method, such as shallow flows in the catchment and the Manning's roughness parameters being outside the range of the model for these shallow flows, a strong need for high quality DTM, grid size affecting the flood extent and its magnitude, the flow paths and delayed hydrograph response due to the artificially trapped water in the grids and the high computational time. Zeiger and Hubbart (2021) combined the hydraulic model HEC-RAS (Brunner, 2016) to simulate RoG 2D hydrodynamics at a catchment scale with the SWAT model (Arnold et al., 1998) to get effective rainfall. The results showed that the HEC-RAS model is able to produce realistic simulations of stage hydrograph response when calibrated for each event and highlights the necessity for time-varying friction coefficients to account for the antecedent moisture conditions (AMCs). David and Schmalz (2020) compared the traditional method of coupling hydrological and hydrodynamic models with the RoG approach for flood assessments in a 38 km² catchment. They concluded that the traditional approach produced a better hydrograph, but the RoG approach gave more detailed information in many aspects, such as the origin of the

overland flow, its path, and the floodplain. The study also showed that the RoG approach has much lower computational time than the traditional approach of offline coupling of two separate hydrological and hydraulic models. RoG technique has also been applied for analyzing the use of urban streets and pathways as floodways to route the flood water during extreme events (Skrede et al., 2020). One of the limitations of this technique is that it may not be feasible for a very large catchment because of the high computational time of the hydrodynamic simulations.

HEC-RAS has been presented with various RoG implementations (David & Schmalz, 2021; Krvavica & Rubinić, 2020; Rangari et al., 2019; Zeiger & Hubbart, 2021). In addition, there are several other studies presenting models using RoG such as Flood-Area (Tyrna et al., 2018), Infoworks ICM v.5.5 (Pina et al., 2016), GUAD-2D (Cea & Rodriguez, 2016), PDWave (Leandro et al., 2016), FloodMap (Yu & Coulthard, 2015), Sipson/UIM (Chen et al., 2010), CCHE2D (Jia et al., 2018), MIKE Flood (Hall, 2015), TUFLOW/SOBEK (Clark et al., 2008), TELEMAC-2D (Ligier, 2016). In these studies, RoG has been applied in a variety of catchments such as urban and rural catchments of various sizes, spatial resolutions, and the number of cells in the mesh for different purposes. The studies have shown that RoG technique is able to simulate the hydrology of the catchment to determine the total volume of water as well as the propagation of that water simulating the hydraulic features of the river system which are important in the assessment of the flash flood damages. Also, they show that this technique has lower computational time as compared to the traditional offline coupling of the two separate hydrological and hydraulic models. There have been many studies using integrated hydrologic-hydraulic modeling in medium and large sized catchments (Coulthard et al., 2013; Hankin et al., 2019; Li et al., 2021; Saksena et al., 2019) and in urban areas (Skrede et al., 2020; Zhu et al., 2016). However, presently there is a lack of studies using RoG approach for simulating flash flood peaks in small and steep mountainous catchments, as well as studies testing the limitation of the method and the hydraulic modeling in steep terrain and for operational purposes. There is a clear need for a better understanding of such floods in such topographies, their behavior and how to simulate them to predict their consequence. This is important for better climate adaptation to mitigate future events like those seen in Utvik in Norway in 2017 (Bruland, 2020) and in Kvam, Norway in 2012 and 2013 (Aalstad et al., 2014) and in Ahr, Germany in 2021 (Fekete & Sandholz, 2021).

The objectives of this study are (1) to apply RoG technique in small and steep catchments for reproducing high peak flows and analyze the response of such catchments, and (2) to test and evaluate if the open-source hydrodynamic model TELEMAC-2D can be efficiently used for this purpose and to predict the following water velocities and inundated areas. We show the suitability of this model for fully integrated hydrologic-hydraulic modeling in small mountainous catchments. It has the advantages of both types of models and reduced simulation time as compared to traditionally offline coupled models. The TELEMAC-2D model is used to compute the flood hydrograph and see the corresponding hydraulic effects and a traditional rainfall-runoff model is used to set the baseflow for the TELEMAC-2D simulations.

2 | MATERIALS AND METHODS

2.1 | Study area and input data

There have been many flash flood events in small and steep catchments of Norway in recent years but most of them are ungauged. The catchment chosen for this study has a potential for extreme flash flood events and is one of the few steep, small and gauged catchments in Norway. The Sleddalen catchment located in Møre og Romsdal county in western Norway (Figure 1). The catchment has an elevation drop of 1379 to 77 m over a catchment length of 4.7 km with a mean slope of 26°. The area of the catchment is 10.5 km². The land-cover in the catchment is described in Table 1. Summer and winter precipitation in the catchment is 879 and 1734 mm respectively. The digital elevation model (DEM) for the catchment was downloaded from the Norwegian mapping authority database (www.hoydedata.no) which is based on a topographic LiDAR scan of the area with 10 m × 10 m resolution. Due to non-availability of any nearby precipitation measurement station, precipitation data was extracted from RadPro, a spatially distributed precipitation dataset with 1 km × 1 km resolution based on a merged product of precipitation radar data and gridded precipitation point observations (Engeland et al., 2018). The observed discharge data was downloaded from the database of Norwegian Water Resources and Energy Directorate (www.nve.no) from the station Sleddalen (Station ID: 97.5.0).

2.2 | Models used

Telemac-2D is originally a 2D hydrodynamic model solving shallow water equations. Later versions of

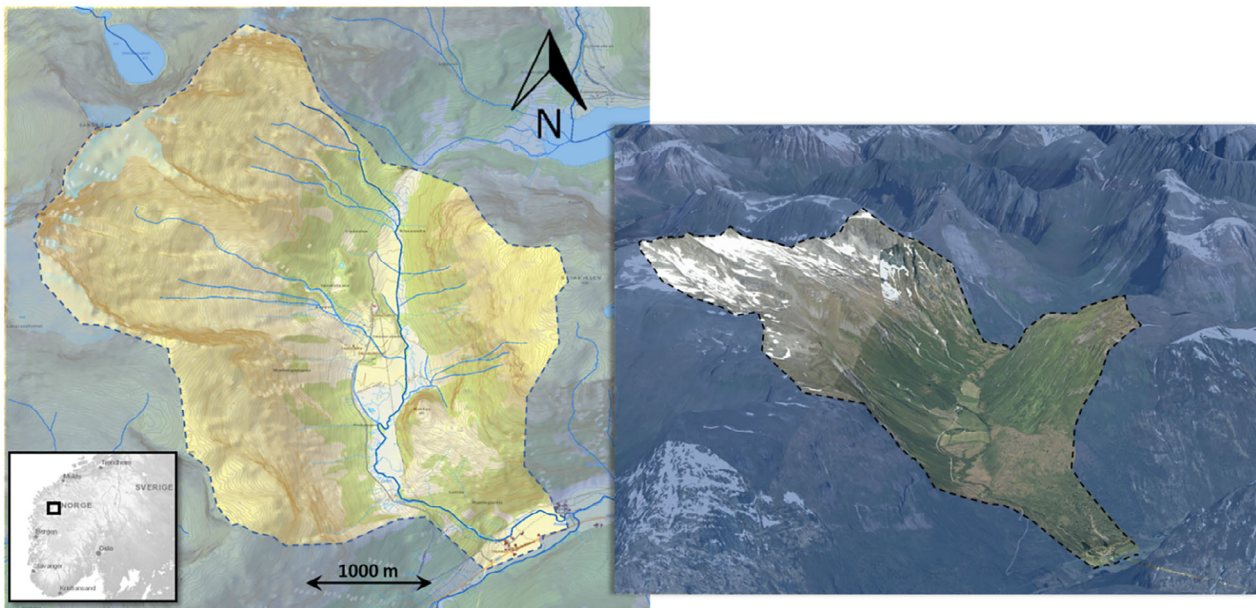


FIGURE 1 Map of study area (left) and aerial photo indicating steepness of the catchment (right).

TABLE 1 Land cover-land use distribution in the catchment.

Description	Area (km ²)	Area (%)
Bare rock and scarce vegetation	4.89	46.57
Forest	2.63	25.05
Open land	2.10	20.00
Swamp	0.38	3.62
Fully cultivated soil	0.34	3.24
Inland pasture	0.09	0.86
River water	0.04	0.38
Urban area	0.02	0.19
Roads	0.01	0.10

TELEMAC-2D (v8p2) have an option to include a hydrological module with RoG technique (Broich et al., 2019; Ligier, 2016). Thus, TELEMAC-2D can simulate the combined overland and river flow for flash floods. Because of the hydraulic part of the model, it is possible to get the hydrograph at any point at any time in the catchment which is useful in determining where and when the situation will be critical along the water courses during extreme events. The model enables to not only evaluate the runoff from each part of the catchment to the river, but also the velocities and shear stress causing erosion or sedimentation combined with the water depths at any part of the river and the catchment. This gives important hydraulic information to evaluate the cause and consequences of flood events such as those reported by Aalstad et al. (2014), Bruland (2020), and Fekete and Sandholz (2021).

The RoG module uses the SCS-CN curve method for runoff calculation (Equation 1). This method is also known as the Natural Resources Conservation Service (NRCS) CN Method developed by USA's Soil Conservation Services (USDA-SCS, 2004). The CN method was developed to estimate the excess precipitation/direct runoff using the storm rainfall depth. Hydrological processes such as infiltration, groundwater recharge, and recession are not considered in the RoG module in TELEMAC-2D. Thus, the model cannot handle the soil and ground water storage and the runoff can be used best only to simulate the peaks of single storms. The relation between surface runoff and infiltrated or "lost" water depends on a dimensionless parameter, the curve number, which is calculated from the hydrologic soil group, land use and AMC in the catchment (USDA-SCS, 2004).

$$Q = \frac{(P - \lambda S)^2}{(P + S - \lambda S)} \text{ when } P \geq I_a \text{ and } \lambda = \frac{I_a}{S}, \quad (1)$$

$$Q = 0, \text{ when } P < I_a$$

where Q is the direct runoff depth, P is the event rainfall depth, I_a is initial abstraction or event rainfall required for the initiation of runoff, λ is the initial abstraction ratio and S is a site storage index defined as the maximum possible difference between P and Q . The rainfall-runoff modeling with SCS-CN method in TELEMAC-2D has been previously used with point rainfall (Ata, 2017; Kelly et al., 2018; Ligier, 2016) and spatially distributed rainfall (Broich et al., 2019) with some enhancement in the model

code. In this study, spatially rainfall is implemented as input directly over the grid cells in the entire catchment. The main input data used for the simulation in TELEMAC-2D are DEM, rainfall, bottom friction, and CN value. Spatially distributed friction coefficients and CN values are used for the current study (Table 2). They were calibrated for each event. More than 90% of the catchment is mainly covered by forest, open land, bare rock, and scarce vegetation. Hence, the CN value for only these land covers were calibrated (Table 3, grayed cells) and other were kept constant when the distributed curve numbers were used for the simulations. Since the calibration of TELEMAC-2D is manual and computationally expensive, we also simulated the same events using a single CN value for the entire catchment to see if it can give satisfactory results. Averaged values of CN were also used because the required soil data were not available to calculate the distributed CN values in the catchment, which is the case in many other similar catchments. The land cover data for the catchment was downloaded from the database of Norwegian Mapping Authority (www.kartverket.no). The input files were prepared using Bluekenue software (Barton, 2019). Bluekenue (3.3.4) and QGIS (3.16) were used for the post processing of the simulation result files and generating the velocity and water depth graphs.

The default value of initial abstraction ratio ($\lambda = 0.2$) was used inside the model. The mean and maximum slopes in the catchment are 0.5 and 5.2 m/m. Since the catchment is very steep, it was important to consider the effect of steep slope. Hence, the correction for steep slope was applied in TELEMAC-2D as per Equation 2 (Huang et al., 2006). Inside the model, the CN value is adjusted

for the steep slope using the formula introduced by Huang et al. (2006):

$$CN(II)_\alpha = CN(II) \frac{(322.79 + 15.63\alpha)}{(\alpha + 323.52)}, \quad (2)$$

where CN(II) is the CN value for normal antecedent moisture condition (AMC II), α is the terrain slope in m/m and varies from 0.14 to 1.4 m/m. The CN(II) values can be raised by up to 6% for $\alpha = 1.4$ (Ligier, 2016). As TELEMAC-2D does not return the abstracted water to the system, the model is used only to simulate single storm events in this study. For operational use in forecasting and planning, it is necessary to combine the RoG simulation in TELEMAC-2D with another model to get realistic hydrological conditions in the catchment prior to flood events. For this purpose, the rainfall-runoff model HBV (Bergström & Forsman, 1973) was used for the design storm simulation. The HBV model was calibrated to the observed discharge for Sleddalen river using the precipitation data from the gridded timeseries RadPro.

3 | RESULTS

A total of seven events from the year 2018 to 2021 representing a variety of situations where the quality of precipitation data and runoff data was considered good, were selected for this study (Figure 2). These were used to calibrate the TELEMAC-2D model for different rainfall patterns, base flows and peak flows. The mesh size used for each simulation was 5 m × 5 m for the river up to 100 m × 100 m for the rest of the catchment. Spatially distributed Manning's roughness coefficients and CN values as well as one averaged CN value were used in the catchment. The base flow for each case was set up based on the observed flow. The initialization and evolution of the simulated flood depends on antecedent condition, baseflow, mesh size and roughness, and the CN value. Due to the long computational time, an optimization based on all these parameters was not possible.

3.1 | Hydrodynamic rainfall-runoff modeling in TELEMAC-2D

In the steering file of the TELEMAC-2D simulation, AMC was set to 2 (normal conditions) only. Hence, the CN values were not converted for the different antecedent conditions. Since the 2D hydraulic models were not originally developed for the hydrology of the catchment

TABLE 2 Manning's roughness coefficients for various areal types in the catchment.

Areal type	Manning's roughness coefficient	Sources
Urban area	0.1	Chow (1959)
Roads	0.02	Garrote et al. (2016)
Fully cultivated soil	0.04	Chow (1959)
Inland pasture	0.259	Van der Sande et al. (2003)
Forest	0.2	Van der Sande et al. (2003)
Open land	0.05	O'Brien and Garcia (2009)
Swamp	0.2	Mtamba et al. (2015)
River water	0.04	Chow (1959)
Bare rock and scarce vegetation	0.02	Garrote et al. (2016)

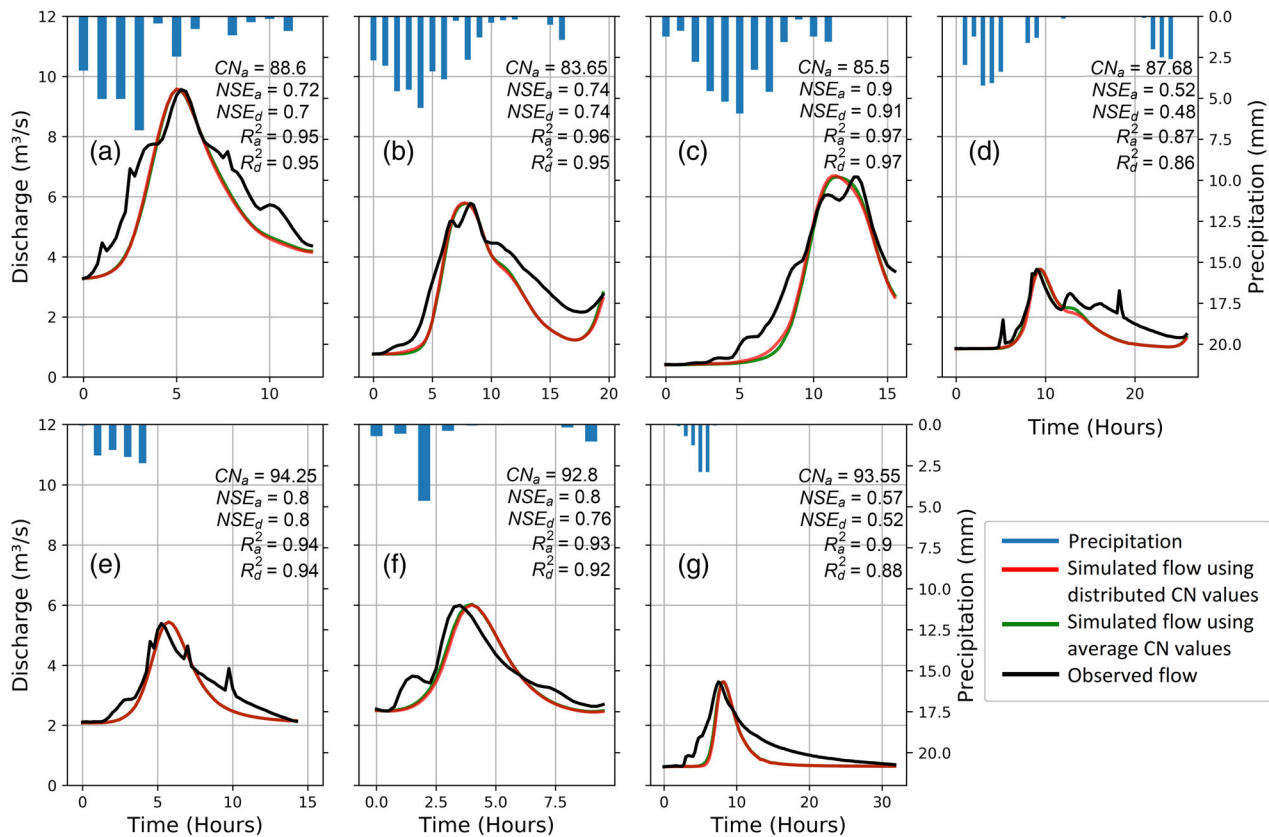


FIGURE 2 Peak flows from rain-on grid simulations in TELEMAC-2D using distributed CN values (red) and using a single averaged CN value (CN_a) (green) compared to observed flow (black), and correlation and Nash Suthcliff model efficiency in case of distributed CN values (R_d^2 , NSE_d) and average CN values (R_a^2 , NSE_a) corresponding to the seven events selected for the current study.

TABLE 3 Calibrated CN values for each event in Figure 2.

Description	Area (%)	Event 2A	2B	2C	2D	2E	2F	2G
Bare rock and scarce vegetation	46.57	91	87	90	90	97	96	95
Forest	25.05	86	78	74	83	93	92	89
Open land	20.00	83	78	79	81	93	90	88
Swamp	3.62	90	90	90	90	90	90	90
Fully cultivated soil	3.24	90	90	90	90	90	90	90
Inland pasture	0.86	89	89	89	89	89	89	89
River water	0.38	100	100	100	100	100	100	100
Urban area	0.19	89	89	89	89	89	89	89
Roads	0.10	91	91	91	91	91	91	91

and very shallow water depths, some parameters can be more sensitive as compared to the case when the model is used only for the hydraulics of the river which is the original field of application of such models (David & Schmalz, 2021). Hence, it is important to check the effect of the model parameters before using the model. In this study, effects of the following parameters were analyzed from the simulation results: (a) CN value, (b) AMCs in the catchment, (c) mesh resolution, and (d) roughness coefficients.

3.2 | Sensitivity analysis

3.2.1 | Curve number

The sensitivity of various values of CN values from 30 to 100 were tested keeping the values of all the other parameters constant. The values lower than 30 had a negligible effect on the runoff volume, hence was not used to test the sensitivity. The results showed that the runoff volume (Figure 3a) is very sensitive to the CN value.

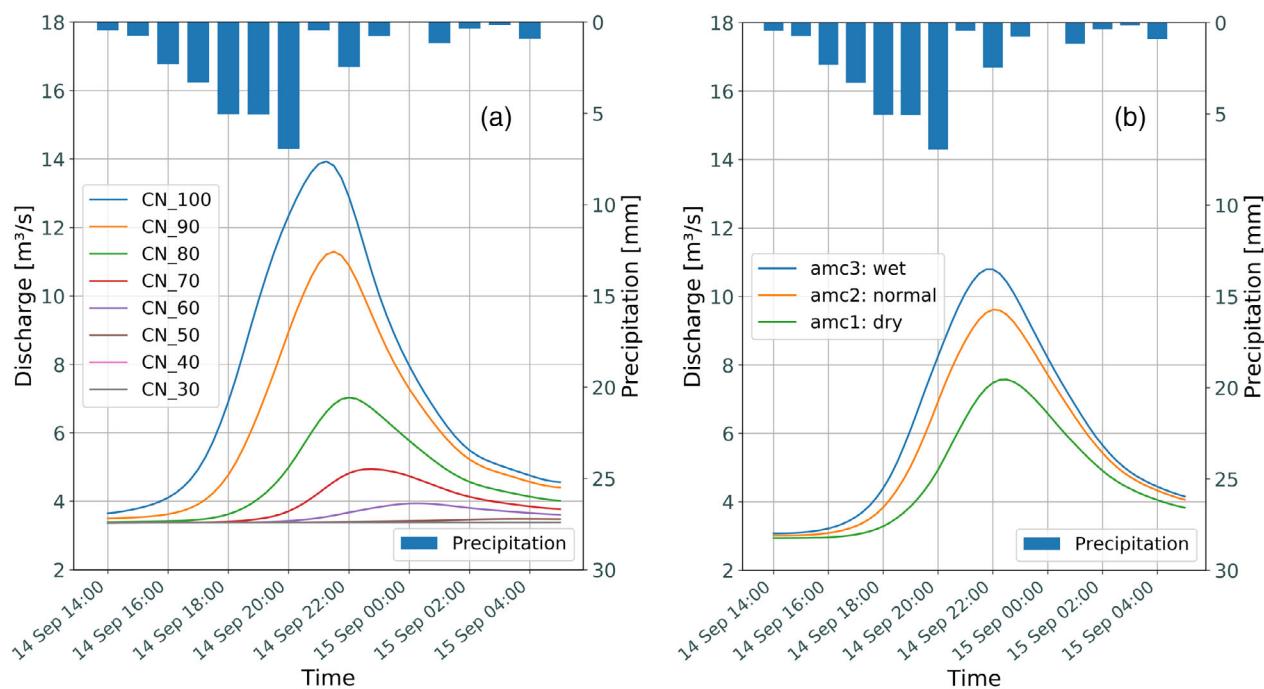


FIGURE 3 Simulated peak flows for the same event where only CN values are varied (a) and where only the antecedent moisture conditions are varied (b).

3.2.2 | Antecedent moisture condition

There is a significant difference in the runoff volume for the three classes of the AMCs (Figure 3b). The formula used for converting CN values for normal AMC to CN values for wet and dry AMC conditions was used as per described by Chow et al. (1988) and Hjelmfelt (1991).

3.2.3 | Roughness

Roughness of the terrain influences the water retained in the catchment and thus it has an influence on the output flood hydrograph. To test the sensitivity to the roughness, the model was tested for different roughness values based on the land use types in the catchment from the literature. The results showed that when the roughness was higher, more water remained in the domain hence less water goes out through the measurement cross-section leading to the reduced peak of the hydrograph in the hydrograph and vice-versa.

3.2.4 | Mesh resolution

To make the simulations faster, a coarser mesh was used in the hill slopes than in the river. Various mesh sizes for the river and the rest of the catchment were evaluated to check

TABLE 4 Applied mesh sizes along the river and for the catchment.

Scenario	Mesh size in river	Mesh size in the rest of the catchment
1	3 m × 3 m	5 m × 5 m
2	5 m × 5 m	100 m × 100 m
3	5 m × 5 m	500 m × 500 m
4	10 m × 10 m	500 m × 500 m

Note: Scenario 2 (marked green) is used in the study.

its sensitivity (Table 4). The results showed that the mesh size was an influential parameter for runoff volume. The coarser the mesh resolution, the lower the runoff volume.

3.3 | Hydrologic modeling in HBV for calculating base flow in TELEMAC-2D simulations

The HBV model was established for Sleddalen catchment and calibrated and run on hourly resolution with the gridded RadPro precipitation data and temperature data from Sleddalen station. The precipitation in each grid cell within the catchment was averaged to the catchment altitudes. The calibration was done for the period with available Radpro data for Sleddalen, September 2018 to

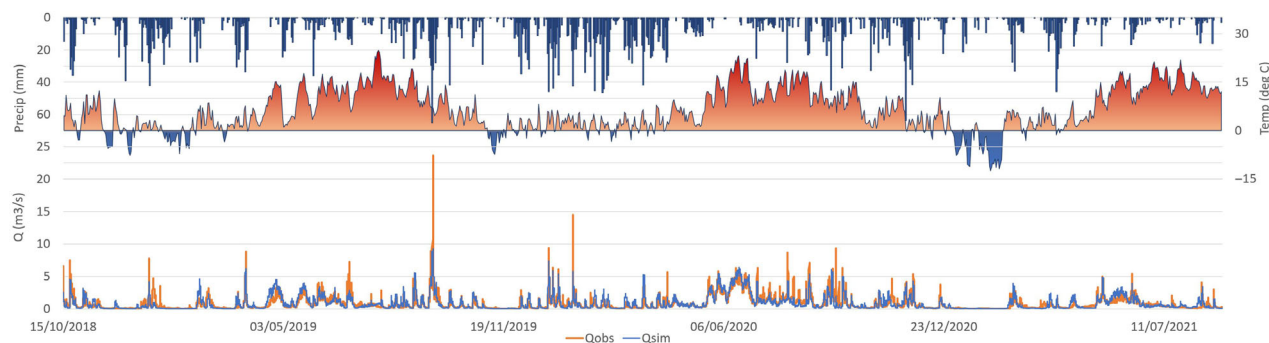


FIGURE 4 Precipitation and temperature input data to the HBV model (upper) and the resulting simulated runoff compared to observed for Sleddalen catchment (lower).

September 2021. The calibration gave a Nash-Sutcliffe— R^2 of 0.70. For the validation period from 2013 to 2018, Radpro data was not available and precipitation input was taken from the Met Office's observations at Kroken, Stryn in Norway about 20 km south-southeast of Sleddalen. R^2 for the validation period was 0.51 which is satisfactory considering the less representative precipitation data. As Figure 4 shows the model reproduced the base flow quite well but under-predicted the peak flows, this was the case both in the calibration and the validation period. The inability to catch the peaks is most likely due to higher precipitation intensities in reality than what RadPro and observations shows. Considering the strong topographical variation in the region and the poor density of precipitation observations, a R^2 of 0.7 and even of 0.5 was satisfactory and since the purpose of the HBV model in this study is to get a relevant base flow to initialize TELEMAC-2D, the calibrated model is considered suitable for the purpose.

3.4 | Design storm

The HBV model was also used to find the most critical combination of design storms with different durations and 200 year return period and the preceding conditions to evaluate the dimensioning 200-year flood design flood according to the national regulations (DiBK, 2017). A 200-year design precipitation was constructed for durations from 1 to 24 h using the intensity-duration-frequency curves downloaded from the database of Norwegian Center for Climate Services (NCCS) (klimaservisesenter.no). Six design precipitation cases (60, 120, 180, 360, 720, and 1440 min duration) with total volumes between 20 mm for 1 h and 147 mm for 24 h, were run superimposed over observed data for the period from 2018 to 2021 and a 200-year flood event in this period was found to be between 20 and 25 m^3/s with the HBV model when snow was not present. A duration of

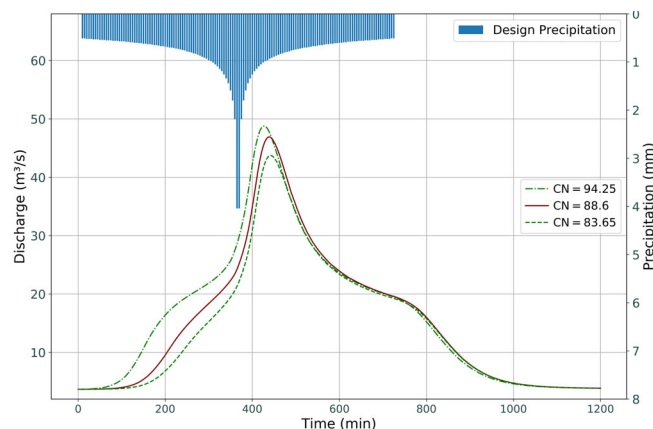


FIGURE 5 200-year design storm runoff from a 12-h design precipitation with a high (94.25), the best fit (88.6), and a low (83.65) curve number (CN) from the calibration to selected events.

between 12 and 24 h gave the highest discharges. The effect of snowmelt was included by using max observed daily average temperature for the simulated day combined with a design precipitation. This combination gave the highest peak flow up to 29 m^3/s . As it is likely that snowmelt can saturate the soils prior to an extreme rain event but not necessarily contribute significantly to the flood, the base flow from the HBV model and AMC prior to this event were used to initialize the design flood simulation in TELEMAC-2D.

The design storm was simulated in TELEMAC-2D using the highest (CN = 94.25), the lowest (CN = 83.65) and the CN value that gave the best fit for the highest observed discharge in the calibration (CN = 88.6) (Figure 5). The resulting hourly maximum discharges ranged from 42 m^3/s for the lowest CN to 46 m^3/s for the highest CN for 12-h duration and from 37 to 39 m^3/s for a 24-h duration. In both the cases, there is a significant difference in the discharge prior to the peak. Higher infiltration at lower CN decreases the discharges in the early stage of the event with between 7 and 10 m^3/s . Figure 6

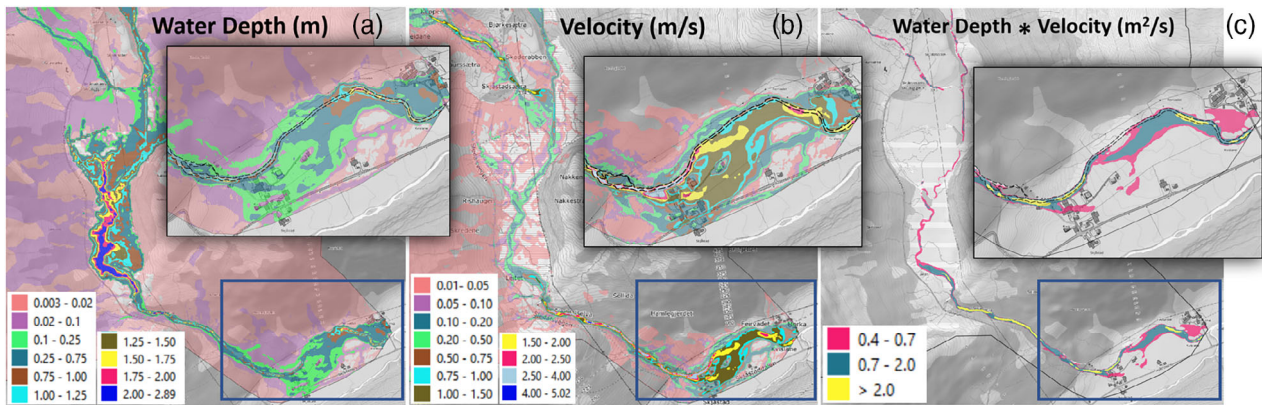


FIGURE 6 Water depth (a) deeper than 0.1 m and velocities (b) higher than 0.25 m/s, and the product of depth and velocity (c) higher than critical levels for pedestrians ($0.4 \text{ m}^2/\text{s}$), vehicles ($0.7 \text{ m}^2/\text{s}$), and buildings ($2 \text{ m}^2/\text{s}$) for the design storm with 200-year return period.

shows the velocity, water depth and the product of depth and velocity in the region of the catchment with the highest damage and consequence potential for the 200-year design storm based on $CN = 88.6$. The highest velocity is 2.54 m/s, the deepest area is 1.77 m deep and the depth-velocity product is up to $11.32 \text{ m}^2/\text{s}$.

4 | DISCUSSION

In this study, we used TELEMAC-2D to simulate flood discharges in a small and steep catchment in Norway. The model was calibrated on seven observed floods and were found to give good results. The results show how the model provides both the peak flood and information relevant for estimation of its consequences in and along the river like flooded areas and critical water velocity. The hydrodynamic model also simulates the residual flow along the river which is usually difficult to estimate in the traditional way of offline coupling of the two separate hydrologic and hydrodynamic models. The current study shows the development of source areas and facilitates the user to extract the runoff hydrograph at any point in the catchment at any time-step unlike the traditional hydrologic model or hydrodynamic model with one source input.

4.1 | Curve number

The calibration results indicate that the CN increases with decreasing flood size in contradiction to what could be expected (Hjelmfelt, 1991). This can be explained by an increasing CN reducing the simulated infiltration and compensating for the lack of subsurface discharge of infiltrated water to the river. At higher discharges, this compensation is less important as in reality a relatively

smaller portion of the discharge originates from infiltrated water. This also influences the simulation of the recession limb (e.g., Figure 2d,h) and the duration and total volume of water in the floods. In turn, this can lead to underestimation of consequences caused by longer duration and higher volumes such as increased erosion and sedimentation volumes, more severe inundation and potential shifts of river course. As the purpose in this study is to investigate and demonstrate the use of RoG to extract important hydraulic properties of floods in a water course related to the peak discharges, the simulation of the recession is considered less important.

The CN method is a widely used method mainly because of its simplicity and because it is based on one parameter. There have been developed many tables in National Engineering Handbook (Section-4) (NEH-4) (USDA-SCS, 2004) for determining CN value for various hydrologic soil groups, land use land covers, and AMCs. Due to limited knowledge about soil covers in the catchment, only one value of CN for the entire catchment was used at first to capture the flow peaks, and because the tabulated CN values have been shown to be inadequate to get the correct runoff volume in many cases (Mishra & Singh, 2006), CN values were calibrated in this study. Nevertheless, there are a wide range of soil covers in the catchment ranging from deep soils to mountainous areas with non or very shallow soil covers, and a more realistic runoff from the catchment is likely if a good relation between these soil covers, CN value and antecedent soil moisture conditions were found and applied. Since this is a small catchment, we were able to calibrate the model using distributed CN values in a reasonable time. This would not be possible in a large catchment because of high computational time.

Another problem with the traditional formula by Chow et al. (1988) and Hjelmfelt (1991) is that there is a sudden jump in the CN while converting it from one

AMC level to another. Mishra and Singh (2006) showed that the exiting criteria of calculating AMC from the cumulative rainfall of the previous 5 days is unrealistic. Some studies have suggested the previous 15 days (Hope & Schulze, 1982) and previous 30 days (Schulze, 1982) of antecedent cumulative rainfall for humid areas and previous 5 days cumulative rainfall in case of arid areas. There was a need for individual calibration for each event because each event had different antecedent rainfall events with different intensities, duration, and distribution. Hence, the CN was calibrated for each event in this study, as also done by Zeiger and Hubbart (2021) in their study. The test of sensitivity shows that the CN and AMC are very critical factors influencing the runoff volume but there was no clear relationship found between the CN and the cumulative rainfall of previous 5-day, base flow or the flow peak in the current study. To investigate this significantly more simulations for more events should be done, but due to the long simulation time this was not conducted in this study. However, in further investigation, the factors which affect the CN value and how to choose a CN value for a particular storm including the impact of base flow and precipitation on the AMC should be studied.

4.2 | Design storm

A 200-year flood was simulated to demonstrate a practical use of the coupling between a continuous hydrological model and RoG in TELEMAC-2D. As AMC and initial base flow are highly important for the simulated peak flow in TELEMAC-2D and since this cannot be simulated realistically by the RoG implementation in TELEMAC-2D, it is necessary to combine TELEMAC-2D with a calibrated hydrological model that provides realistic initial conditions for operational use and to estimate design flood properties. For this purpose, the HBV model was used. The duration giving the highest peak flow was found to be between 12 and 24 h and with total precipitation volumes of 107 and 147 mm respectively.

The HBV model gave an hourly peak discharge of $29 \text{ m}^3/\text{s}$ while the TELEMAC-2D model with the same initial conditions gave a peak discharge up to $47 \text{ m}^3/\text{s}$. Compared to the observations, the HBV model underestimated the peak discharges while TELEMAC-2D simulated a value closer to the peak discharges. There is a difference of up to 10% between the peak flows simulated by the different CN. Even though this is within the uncertainty for flood peak calculations, the calibration indicates that a lower CN gives a better fit at higher flows and thus in these situations a lower CN is probably more

realistic than the highest. The combination between the HBV-model and TELEMAC-2D increases the simulation efficiency and gives more reliable results. A closer coupling between these models would allow for continuous hydrological and hydraulic simulation that have the advantage of integrating antecedent ground and moisture conditions to the flood event (Tsegaw et al., 2020).

4.3 | Roughness

In the current study, distributed values of roughness are used in the catchment. Based on initial values from Chow (1959), the manning numbers can be adjusted to get a better fit of the peaks similar to several previous studies (Garrote et al., 2016; Kalyanapu et al., 2009; Mtamba et al., 2015; Shen et al., 2017; van der Sande et al., 2003). But by doing this, the friction values can possibly become too high for some of the events at shallow water depths (Hall, 2015). It can cause a significant portion of water to get trapped in the domain and even increased CN values will not compensate for this.

4.4 | Mesh resolution

The result of the analysis shows that the mesh resolution can also control the outflow volume. The coarser the mesh resolution, the lower the runoff volume. The use of finer mesh resolution made the simulations computationally more expensive. High performance multi-core super computers can decrease the time for computationally expensive hydrodynamic simulations, but TELEMAC-2D is not compatible for GPU yet, hence, it can only be run on one CPU. The benefit of using coarser mesh was that the computational time was decreased many-fold. But there are some limitations of using a coarser mesh. The flow generated from the rainfall migrates downstream by solving the shallow water equations in the hydrodynamic model. Here, the water depths are too shallow on the flat and large cells of $100 \text{ m} \times 100 \text{ m}$ before this water joins a stream. The manning's friction coefficient is often too large for these shallow water depths that water at these depths get trapped in the roughness and thus affect the actual water-flow propagation time. Neither does a coarse grid represent the true geometry of the catchment, and this might also cause more water to stay in the domain showing lower peaks as compared to simulations where finer mesh is used. This needs to be considered while planning the model. The results show that the mesh resolution is one of the controlling factors for outflow volume. These results are in coherence with the results from the study by Clark et al. (2008) where it was

shown that the model results were very sensitive to the changes in grid-sizes.

4.5 | Equifinality

During the calibration process of the events, it was found that different combinations of the Manning's friction coefficient and CN gave equally acceptable results as well as the different combinations of the spatially distributed CN values. This phenomenon, called equifinality, is addressed by Beven (2012). High initial moisture conditions (high AMC) which hydrologically should give high discharge can be compensated with a high infiltration (low CN) reducing the runoff to get a good fit. This effect is probably the explanation for the calibration giving lower CN at higher observed runoff. Similarly, the roughness influences retention of water in the catchment and too high roughness can be compensated with unrealistically high CN. An improved and more physically correct hydrological module including soil moisture variability and subsurface outflow in TELEMAC-2D could possibly reduce the challenging equifinality in this case. Also, a Monte Carlo optimization including all the parameters could give a more physically correct model. Due to the long simulation time this was not achievable in this study.

Despite the limitations mentioned above, the procedure used in the paper still serves the purpose of simulating the hydrology of such a steep catchment to determine the volume of water as well as the propagation of that water simulating the hydraulic features of the river system which are important in the assessment of the flash flood damages. Similar study has not been done yet as per our knowledge in such a small and steep catchment having an average slope of 26°. RoG model like demonstrated here, gives realistic inflow to any point along the water course and will be a more realistic approach for identifying critical locations where a flood has high potential for creating local or downstream damages as compared to a traditional hydraulic or hydrological model alone. It also provides water velocities and depth along the water courses, in tributaries and in the inundated areas at any time in addition to the discharges. This feature makes it a suitable tool for assessing the erosion and sedimentation during a flood and related challenges (Moraru et al., 2021) and thus, the combined effect of water depth and velocities as addressed in the national regulation act (DiBK, 2017), by Kreibich et al. (2009) and by Shand et al. (2011).

The results can be used by planners and decision makers for optimizing mitigation measures and to get correct dimensioning criteria for infrastructure and areal

planning. The results can also be helpful for contingency people to be better prepared beforehand the extreme events with better and more precise flood forecasting including the scenarios for local consequences and potential mitigation measures to reduce the damages during the event.

5 | CONCLUSION

This study focuses on an approach to reproduce the flash flood peaks in small and steep mountainous catchments together with representing the consequences of the flash flood in the entire catchment in terms of water depths and high velocities. This is important knowledge in areal and infrastructure planning processes, for optimizing mitigation measures and for adapting to the climate changes. TELEMAC-2D model is used in the current study as an integrated hydrologic-hydrodynamic toolbox. The rainfall was directly applied as input over the entire catchment which is called DRM or RoG technique. A total of seven events caused by rainfall of different characteristics were reproduced for the high flows during the summers of the years 2018 to 2021. The results show a good correlation between the observed and simulated flood peaks with correlation coefficient (R^2) ranging from 0.97 to 0.87. Combined with the HBV-model, it is shown that TELEMAC-2D can be an efficient tool for estimating realistic design floods and their corresponding water depths and velocities along the water course, in the tributaries and in the entire catchment. Such results will provide a tool for contingency planner and crisis management for identification of critical locations for people, buildings and infrastructure during a flood, a better tool for areal planners and infrastructure owners in their risk and vulnerability analysis and for decision makers to identify the optimal socio-economic solution in the societal adaptation to climate change scenarios.

DATA AVAILABILITY STATEMENT

The data that support the findings of this study are available from the corresponding author upon reasonable request.

ORCID

Nitesh Godara  <https://orcid.org/0000-0003-2906-3649>

REFERENCES

- Aalstad, G. H., Berg, H., & Helgaas, G. (2014). *The flood protection concept in Kvam, Norway*. 1, 2–3.
- Adnan, M. S. G., Dewan, A., Zannat, K. E., & Abdullah, A. Y. M. (2019). The use of watershed geomorphic data in flash flood susceptibility zoning: A case study of the Karnaphuli and Sangu

- river basins of Bangladesh. *Natural Hazards*, 99(1), 425–448. <https://doi.org/10.1007/s11069-019-03749-3>
- Arnold, J. G., Srinivasan, R., Muttiah, R. S., & Williams, J. R. (1998). Large area hydrologic modeling and assessment part I: Model development. *JAWRA Journal of the American Water Resources Association*, 34(1), 73–89. <https://doi.org/10.1111/J.1752-1688.1998.TB05961.X>
- Ata, R. (2017). *Telemac2d user manual. Version 7.2.*
- Barton, A. J. (2019). Blue Kenue enhancements from 2014 to 2019. <https://doi.org/10.5281/zenodo.3611511>
- Bergström, S., & Forsman, A. (1973). *Sveriges Meteorologiska och Hydrologiska Institut Development of a conceptual deterministic rainfall - runoff model.*
- Beven, K. (2012). Rainfall-runoff modelling. In *Rainfall-runoff modelling*. Wiley. <https://doi.org/10.1002/9781119951001>
- Boithias, L., Sauvage, S., Lenica, A., Roux, H., Abbaspour, K. C., Larnier, K., Dartus, D., & Sánchez-Pérez, J. M. (2017). Simulating flash floods at hourly time-step using the SWAT model. *Water (Switzerland)*, 9(12), 1–25. <https://doi.org/10.3390/w9120929>
- Broich, K., Pflugbeil, T., Disse, M., & Nguyen, H. (2019). Using TELEMAC-2D for hydrodynamic modeling of rainfall-runoff. *XXVith Telemac & Mascaret User Club, October.*
- Bruland, O. (2020). How extreme can unit discharge become in steep Norwegian catchments? *Hydrology Research*, 51(2), 290–307. <https://doi.org/10.2166/nh.2020.055>
- Brunner, G. W. (2016). *HEC-RAS river analysis system 2D modeling user's manual.*
- Bryndal, T., Franczak, P., Krocak, R., Cabaj, W., & Kołodziej, A. (2017). The impact of extreme rainfall and flash floods on the flood risk management process and geomorphological changes in small Carpathian catchments: A case study of the Kasiniczanka river (Outer Carpathians, Poland). *Natural Hazards*, 88(1), 95–120. <https://doi.org/10.1007/s11069-017-2858-7>
- Cea, M., & Rodriguez, M. (2016). Two-dimensional coupled distributed hydrologic-hydraulic model simulation on watershed. *Pure and Applied Geophysics*, 173(3), 909–922. <https://doi.org/10.1007/s00024-015-1196-5>
- Chen, A. S., Djordjević, S., Leandro, J., & Savić, D. A. (2010). An analysis of the combined consequences of pluvial and fluvial flooding. *Water Science and Technology*, 62(7), 1491–1498. <https://doi.org/10.2166/wst.2010.486>
- Chow, V. T. (1959). Open channel hydraulics. In *Open channel hydraulics*. Elsevier.
- Chow, V. T., Maidment, D. R., & Mays, L. W. (1988). *Applied Hydrology Chow_1988.pdf*. (pp. 1–294). http://ponce.sdsu.edu/Applied_Hydrology_Chow_1988.pdf
- Clark, K., Ball, J., & Babister, K. (2008). Can fixed grid 2 hydraulic models be used as hydrologic models? *Proceedings of Water Down Under, 2008*, 2496–2507.
- Costache, R., Barbulescu, A., & Pham, Q. (2021). Integrated framework for detecting the areas prone to flooding generated by flash-floods in small river catchments. *Water*, 13(6), 758. <https://doi.org/10.3390/w13060758>
- Costache, R., Tin, T. T., Arabameri, A., Crăciun, A., Costache, I., Islam, A. R. M. T., Sahana, M., & Pham, B. T. (2022). Stacking state-of-the-art ensemble for flash-flood potential assessment. *Geocarto International*, 1–27, 13812–13838. <https://doi.org/10.1080/10106049.2022.2082558>
- Coulthard, T. J., Neal, J. C., Bates, P. D., Ramirez, J., de Almeida, G. A. M., & Hancock, G. R. (2013). Integrating the LISFLOOD-FP 2D hydrodynamic model with the CAESAR model: Implications for modelling landscape evolution. *Earth Surface Processes and Landforms*, 38(15), 1897–1906. <https://doi.org/10.1002/esp.3478>
- David, A., & Schmalz, B. (2020). Flood hazard analysis in small catchments: Comparison of hydrological and hydrodynamic approaches by the use of direct rainfall. *Journal of Flood Risk Management*, 13(4), 1–26. <https://doi.org/10.1111/jfr3.12639>
- David, A., & Schmalz, B. (2021). A systematic analysis of the interaction between rain-on-grid-simulations and spatial resolution in 2d hydrodynamic modeling. *Water (Switzerland)*, 13(17), 2346. <https://doi.org/10.3390/w13172346>
- DiBK. (2017). *Veiledning om tekniske krav til byggverk (TEK17, Issue July)*. <https://dibk.no/regelverk/byggteknisk-forskrift-tek17>
- Engeland, K., Abdella, S. Y., Azad, R., Arrturi Elo, C., Lussana, C., Tadege Mengistu, Z., Nipen, T., & Randriamampianina, R. (2018). Use of precipitation radar for improving estimates and forecasts of precipitation estimates and streamflow. *20th EGU General Assembly, In EGU General Assembly Conference Abstracts*, 12207.
- Fekete, A., & Sandholz, S. (2021). *Here comes the flood, but not failure? Lessons to learn after the heavy rain and pluvial floods in Germany 2021 science-based support to the Sendai framework for disaster risk reduction view project INCREASE: Inclusive and integrated multi-hazard risk man.* <https://doi.org/10.3390/w13213016>
- Felder, G., Zischg, A., & Weingartner, R. (2017). The effect of coupling hydrologic and hydrodynamic models on probable maximum flood estimation. *Journal of Hydrology*, 550, 157–165. <https://doi.org/10.1016/j.jhydrol.2017.04.052>
- Garrote, J., Alvarenga, F. M., & Díez-Herrero, A. (2016). Quantification of flash flood economic risk using ultra-detailed stage-damage functions and 2-D hydraulic models. *Journal of Hydrology*, 541, 611–625. <https://doi.org/10.1016/j.jhydrol.2016.02.006>
- Gaume, E., Bain, V., Bernardara, P., Newinger, O., Barbuc, M., Bateman, A., Blaškovičová, L., Blöschl, G., Borga, M., Dumitrescu, A., Daliakopoulos, I., Garcia, J., Irimescu, A., Kohnova, S., Koutroulis, A., Marchi, L., Matreata, S., Medina, V., Preciso, E., ... Viglione, A. (2009). A compilation of data on European flash floods. *Journal of Hydrology*, 367(1–2), 70–78. <https://doi.org/10.1016/j.jhydrol.2008.12.028>
- Hall, J. (2015). Direct rainfall flood modelling: The good, the bad and the ugly. *Australian Journal of Water Resources*, 19(1), 74–85. <https://doi.org/10.7158/13241583.2015.11465458>
- Hankin, B., Metcalfe, P., Beven, K., & Chappell, N. A. (2019). Integration of hillslope hydrology and 2D hydraulic modelling for natural flood management. *Hydrology Research*, 50(6), 1535–1548. <https://doi.org/10.2166/nh.2019.150>
- Hjelmfelt, A. T. (1991). Investigation of curve number procedure. *Journal of Hydraulic Engineering*, 117(6), 725–737. [https://doi.org/10.1061/\(ASCE\)0733-9429\(1991\)117:6\(725\)](https://doi.org/10.1061/(ASCE)0733-9429(1991)117:6(725))
- Hope, A. S., & Schulze, R. E. (1982). Improved estimates of storm-flow volumes using the SCS curve number method. In V. P. Singh (Ed.), *Rainfall-runoff relationships* (pp. 419–431). Water Resources Publications.
- Hu, P., Zhang, Q., Shi, P., Chen, B., & Fang, J. (2018). Flood-induced mortality across the globe: Spatiotemporal pattern and

- influencing factors. *Science of the Total Environment*, 643, 171–182. <https://doi.org/10.1016/j.scitotenv.2018.06.197>
- Huang, M., Gallichand, J., Wang, Z., & Goulet, M. (2006). A modification to the soil conservation service curve number method for steep slopes in the Loess Plateau of China. *Hydrological Processes*, 20(3), 579–589. <https://doi.org/10.1002/hyp.5925>
- Jia, Y., Shirmeen, T., Locke, M. A., Lizotte, R. E., Jr., & Douglas Shields, F., Jr. (2018). Simulation of surface runoff and channel flows using a 2D numerical model. In *Soil erosion - rainfall erosivity and risk assessment*. IntechOpen. <https://doi.org/10.5772/intechopen.80214>
- Kalyanapu, A. J., Burian, S. J., & McPherson, T. N. (2009). Effect of land use-based surface roughness on hydrologic model output. *Journal of Spatial Hydrology*, 9, 2. <https://scholarsarchive.byu.edu/josh/vol9/iss2/2>
- Kayan, G., Riazi, A., Erten, E., & Türker, U. (2021). Peak unit discharge estimation based on ungauged watershed parameters. *Environmental Earth Sciences*, 80(1), 1–10. <https://doi.org/10.1007/s12665-020-09317-4>
- Kelly, D. M., Ata, R., & Li, Y. (2018). Modification of TELEMAC 2D for storm surge use. *The XXVth TELEMASCARET User Conference*, 4–10. <https://hdl.handle.net/20.500.11970/105193>
- Kreibich, H., Piroth, K., Seifert, I., Maiwald, H., Kunert, U., Schwarz, J., Merz, B., & Thieken, A. H. (2009). Is flow velocity a significant parameter in flood damage modelling? *Natural Hazards and Earth System Science*, 9(5), 1679–1692. <https://doi.org/10.5194/nhess-9-1679-2009>
- Krvavica, N., & Rubinić, J. (2020). Evaluation of design storms and critical rainfall durations for flood prediction in partially urbanized catchments. *Water (Switzerland)*, 12(7), 2044. <https://doi.org/10.3390/w12072044>
- Leandro, J., Schumann, A., & Pfister, A. (2016). A step towards considering the spatial heterogeneity of urban key features in urban hydrology flood modelling. *Journal of Hydrology*, 535, 356–365. <https://doi.org/10.1016/j.jhydrol.2016.01.060>
- Li, Z., Chen, M., Gao, S., Luo, X., Gourley, J. J., Kirstetter, P., Yang, T., Kolar, R., McGovern, A., Wen, Y., Rao, B., Yami, T., & Hong, Y. (2021). CREST-iMAP v1.0: A fully coupled hydrologic-hydraulic modeling framework dedicated to flood inundation mapping and prediction. *Environmental Modelling and Software*, 141(April), 105051. <https://doi.org/10.1016/j.envsoft.2021.105051>
- Ligier, P. (2016). *Implementation of a rainfall-runoff model in TELEMAC-2D*. <https://hdl.handle.net/20.500.11970/104541>
- Merz, B., Blöschl, G., Vorogushyn, S., Dottori, F., Aerts, J. C. J. H., Bates, P., Bertola, M., Kemter, M., Kreibich, H., Lall, U., & Macdonald, E. (2021). Causes, impacts and patterns of disastrous river floods. *Nature Reviews Earth & Environment*, 2(9), 592–609. <https://doi.org/10.1038/s43017-021-00195-3>
- Merz, B., Kreibich, H., Schwarze, R., & Thieken, A. (2010). Review article “assessment of economic flood damage.”. *Natural Hazards and Earth System Science*, 10(8), 1697–1724. <https://doi.org/10.5194/nhess-10-1697-2010>
- Mishra, S. K., & Singh, V. P. (2006). A relook at NEH-4 curve number data and antecedent moisture condition criteria. *Hydrological Processes*, 20(13), 2755–2768. <https://doi.org/10.1002/hyp.6066>
- Moraru, A., Pavliček, M., Bruland, O., & Rütther, N. (2021). The story of a Steep River: Causes and effects of the flash flood on 24 July 2017 in Western Norway. *Water*, 13(12), 1688. <https://doi.org/10.3390/W13121688>
- Mtamba, J., van der Velde, R., Ndomba, P., Zoltán, V., & Mtaló, F. (2015). Use of Radarsat-2 and Landsat TM images for spatial parameterization of Manning's roughness coefficient in hydraulic modeling. *Remote Sensing*, 7(1), 836–864. <https://doi.org/10.3390/rs70100836>
- Nguyen, P., Thorstensen, A., Sorooshian, S., Hsu, K., AghaKouchak, A., Sanders, B., Koren, V., Cui, Z., & Smith, M. (2016). A high resolution coupled hydrologic-hydraulic model (HiResFlood-UCI) for flash flood modeling. *Journal of Hydrology*, 541, 401–420. <https://doi.org/10.1016/j.jhydrol.2015.10.047>
- O'Brien, J. S., & Garcia, R. (2009). FLO-2D Reference manual. www.flo-2d.com, 595.
- Pina, R. D., Ochoa-Rodriguez, S., Simões, N. E., Mijic, A., Marques, A. S., & Maksimović, Č. (2016). Semi- vs. fully-distributed urban stormwater models: Model set up and comparison with two real case studies. *Water (Switzerland)*, 8(2), 58. <https://doi.org/10.3390/w8020058>
- Rangari, V. A., Umamahesh, N. V., & Bhatt, C. M. (2019). Assessment of inundation risk in urban floods using HEC RAS 2D. *Modeling Earth Systems and Environment*, 5(4), 1839–1851. <https://doi.org/10.1007/s40808-019-00641-8>
- Roald, L. A. (2019). *Floods in Norway*. https://publikasjoner.nve.no/rapport/2021/rapport2021_01.pdf
- Saharia, M., Kirstetter, P.-E., Vergara, H., Gourley, J. J., Hong, Y., & Giroud, M. (2017). Mapping flash flood severity in the United States. *Journal of Hydrometeorology*, 18(2), 397–411. <https://doi.org/10.1175/JHM-D-16-0082.1>
- Saksena, S., Merwade, V., & Singhofen, P. J. (2019). Flood inundation modeling and mapping by integrating surface and subsurface hydrology with river hydrodynamics. *Journal of Hydrology*, 575, 1155–1177. <https://doi.org/10.1016/j.jhydrol.2019.06.024>
- Schulze, R. E. (1982). The use of soil moisture budgeting to improve stormflow estimates by the SCS curve number method. In *University of Natal, Department of Agricultural Engineering, Report 15, Pietermaritzburg*.
- Seneviratne, S. I., Zhang, X., Adnan, M., Badi, W., Dereczynski, C., Di Luca, A., Ghosh, S., Iskandar, I., Kossin, J., Lewis, S., Otto, F., Pinto, I., Satoh, M., Vicente-Serrano, S. M., Wehner, M., & Zhou, B. (2021). *IPCC - climate change 2021: The physical science basis - chapter 11: Weather and climate extreme events in a changing climate* (p. 1610). Cambridge University Press. <https://doi.org/10.1017/9781009157896.013>
- Shand, T., Smith, G., Cox, R., & Blacka, M. (2011). Development of Appropriate Criteria for the Safety and Stability of Persons and Vehicles in Floods. *Proceedings of the 34th World Congress of the International Association for Hydro- Environment Research and Engineering: 33rd Hydrology and Water Resources Symposium and 10th Conference on Hydraulics in Water Engineering, Brisbane, Australia, 26 June–1 July, 9*.
- Shen, Y., Goodall, J. L., & Chase, S. B. (2017). Method for rapidly assessing the overtopping risk of bridges due to flooding over a large geographic region. *JAWRA Journal of the American Water Resources Association*, 53(6), 1437–1452. <https://doi.org/10.1111/1752-1688.12583>
- Skrede, T. I., Muthanna, T. M., & Alfredesen, K. (2020). Applicability of urban streets as temporary open floodways. *Hydrology Research*, 51(4), 621–634. <https://doi.org/10.2166/NH.2020.067>

- Smith, D. I. (1994). Flood damage estimation—a review of urban stage-damage curves and loss functions. *Water SA*, 20(3), 231–238. https://hdl.handle.net/10520/AJA03784738_1124
- Trigo, R. M., Ramos, C., Pereira, S. S., Ramos, A. M., Zêzere, J. L., & Liberato, M. L. R. (2016). The deadliest storm of the 20th century striking Portugal: Flood impacts and atmospheric circulation. *Journal of Hydrology*, 541, 597–610. <https://doi.org/10.1016/j.jhydrol.2015.10.036>
- Tsegaw, A. T., Thomas Skaugen, K. A., & Muthanna, T. M. (2020). A dynamic river network method for the prediction of floods using a parsimonious rainfall-runoff model Aynalem Tassechew Tsegaw, Thomas Skaugen, Knut Alfredsen. *Hydrology Research*, 51, 146–168. <https://doi.org/10.2166/nh.2019.003>
- Tyrna, B., Assmann, A., Fritsch, K., & Johann, G. (2018). Large-scale high-resolution pluvial flood hazard mapping using the raster-based hydrodynamic two-dimensional model FloodAreaHPC. *Journal of Flood Risk Management*, 11, S1024–S1037. <https://doi.org/10.1111/jfr3.12287>
- USDA-SCS. (2004). Part 630 Hydrology National Engineering Handbook Chapter 10 estimation of direct runoff from storm rainfall. In *National Engineering Handbook*. USDA-NRCS (United States Department of Agriculture-Natural Resources Conservation Service).
- van der Sande, C. J., de Jong, S. M., & de Roo, A. P. J. (2003). A segmentation and classification approach of IKONOS-2 imagery for land cover mapping to assist flood risk and flood damage assessment. *International Journal of Applied Earth Observation and Geoinformation*, 4(3), 217–229. [https://doi.org/10.1016/S0303-2434\(03\)00003-5](https://doi.org/10.1016/S0303-2434(03)00003-5)
- WMO. (2021). Water-related hazards dominate disasters in the past 50 years. <https://public.wmo.int/en/media/press-release/water-related-hazards-dominate-disasters-past-50-years>
- Yu, D., & Coulthard, T. J. (2015). Evaluating the importance of catchment hydrological parameters for urban surface water flood modelling using a simple hydro-inundation model. *Journal of Hydrology*, 524, 385–400. <https://doi.org/10.1016/j.jhydrol.2015.02.040>
- Zeiger, S. J., & Hubbart, J. A. (2021). Measuring and modeling event-based environmental flows: An assessment of HEC-RAS 2D rain-on-grid simulations. *Journal of Environmental Management*, 285(February), 112125. <https://doi.org/10.1016/j.jenvman.2021.112125>
- Zhai, X., Zhang, Y., Zhang, Y., Guo, L., & Liu, R. (2021). Simulating flash flood hydrographs and behavior metrics across China: Implications for flash flood management. *Science of the Total Environment*, 763(142), 977. <https://doi.org/10.1016/j.scitotenv.2020.142977>
- Zhu, Z., Oberg, N., Morales, V. M., Quijano, J. C., Landry, B. J., & Garcia, M. H. (2016). Integrated urban hydrologic and hydraulic modelling in Chicago, Illinois. *Environmental Modelling & Software*, 77, 63–70. <https://doi.org/10.1016/j.envsoft.2015.11.014>

How to cite this article: Godara, N., Bruland, O., & Alfredsen, K. (2023). Simulation of flash flood peaks in a small and steep catchment using rain-on-grid technique. *Journal of Flood Risk Management*, 16(3), e12898. <https://doi.org/10.1111/jfr3.12898>